CONFIDENTIAL

OFFICE OF SCIENTIFIC RESEARCH & DEVELOPMENT
NATIONAL DEFENSE RESEARCH COMMITTEE
DIVISION SIX - SECTION 6.1

FORCE TESTS OF THE UNITED SHOE MACHINERY CORP. NO. 8 HYDROBOMB

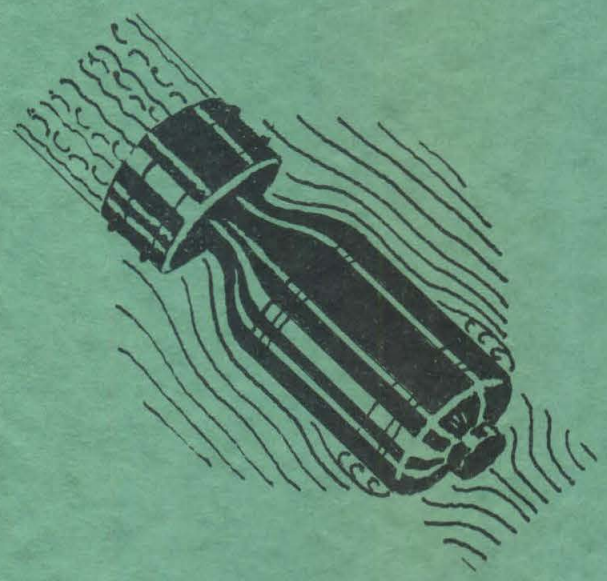

THE HIGH SPEED WATER TUNNEL
CALIFORNIA INSTITUTE OF TECHNOLOGY
PASADENA, CALIFORNIA

SECTION Nº 6.1 sr 207-2247
LABORATORY Nº ND-29.1

CONFIDENTIAL

COPY Nº 117

OFFICE OF SCIENTIFIC RESEARCH AND DEVELOPMENT
NATIONAL DEFENSE RESEARCH COMMITTEE
DIVISION SIX — SECTION 6.1

FORCE TESTS OF THE UNITED SHOE MACHINERY CORPORATION NO. 8 HYDROBOMB

ROBERT T. KNAPP
OFFICIAL INVESTIGATOR

THE HIGH SPEED WATER TUNNEL
AT THE
CALIFORNIA INSTITUTE OF TECHNOLOGY
HYDRODYNAMICS LABORATORY
PASADENA, CALIFORNIA

Section No. 6.1-sr207-2247

Laboratory No. ND-29.1

Report Prepared by
Gerald B. Robison
Hydraulic Engineer

August 25, 1945

TABLE OF CONTENTS

SUMMARY AND CONCLUSIONS

Force and cavitation tests of the United Shoe Machinery Corporation Hydrobomb, Design No. 8, are reported herein. There were two basic models, one having 28-inch fin span for both horizontal and vertical fins, and one with 28-inch vertical and 34-inch horizontal fin span. Seven models were actually tested, namely, one finless, 28-inch and 34-inch fin spans without rings, 28-inch and 34-inch fin spans with 10-degree cone angle rings, and 28-inch and 34-inch fin spans with 5-degree cone angle rings.

CONCLUSIONS

1. Only minor cavitation will be developed at design speed and submergence

2. Rudder effects on cross force, lift, and moment coefficients are several times those of the 30-A design previously tested.

3. The shroud rings on the 28-inch fin span model have the effect of reducing the static instability, so that with zero rudders, the hydrobomb has nearly neutral stability. Rings on the 34-inch fin span model produce a marked static stability which is undesirable for control and maneuverability.

4. The unusually large fin area of these models appears to reduce any advantage of a shroud ring to its possible action in the bubble stage. If one be used, the 10-degree cone angle ring was better than the same ring at 5-degree cone angle, particularly as regards cavitation. Preliminary flow studies with a finless afterbody indicated a 5-degree ring shroud be preferable. That it was not, appears to be due to unusual complexities in the flow pattern produced by the extra large fins and, perhaps, to the ring profile which does not fit the flow at that angle.

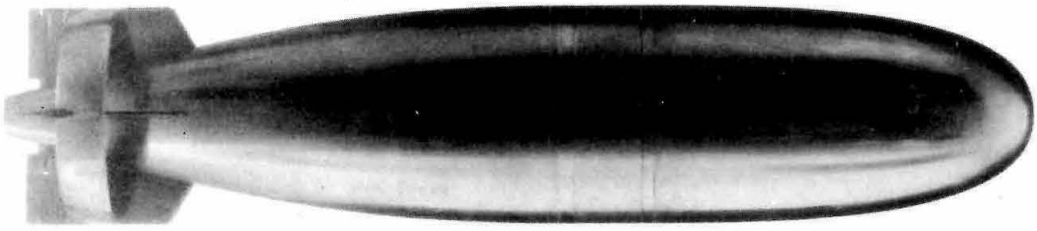

28-INCH FIN SPAN WITH 10-DEGREE CONE ANGLE SHROUD RING

34-INCH HORIZONTAL FIN SPAN WITH 10-DEGREE CONE ANGLE SHROUD RING

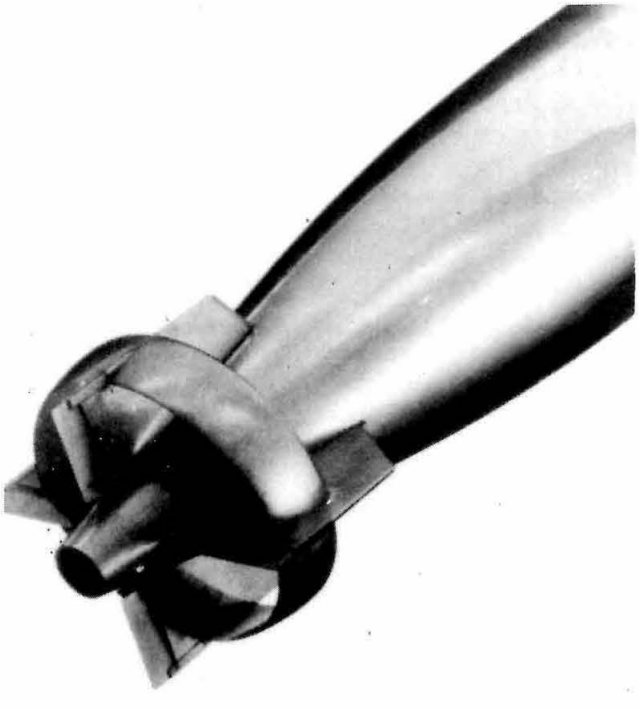

28-INCH FIN SPAN WITH 10-DEGREE CONE ANGLE SHROUD RING

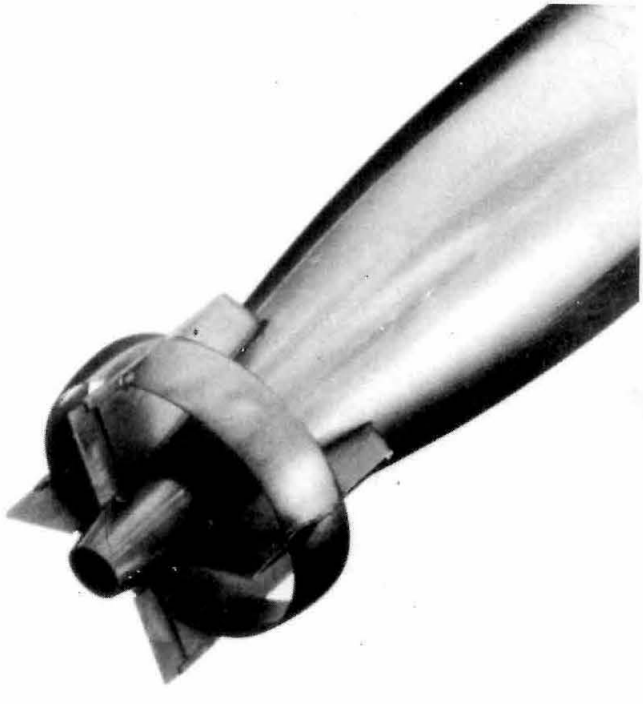

34-INCH HORIZONTAL FIN SPAN WITH 10-DEGREE CONE ANGLE SHROUD RING

FIG. 1 – PHOTOGRAPHS OF 12-INCH DIAMETER MODELS OF HYDROBOMB TESTED IN WATER TUNNEL

FORCE TESTS OF THE UNITED SHOE MACHINERY CORPORATION NO. 8 HYDROBOMB

GENERAL

This report presents the results of tests on the United Shoe Machinery Corporation Hydrobomb, Design No. 8. Two basic models were tested, one in which both horizontal and vertical fins had a 28-inch span, and one in which the vertical fins were 28 inches and the horizontal fins a 34-inch span (prototype dimensions). Views of these models are shown in Figure 1, an outline drawing appears as Figure 2. Nose and afterbody contour data are given under Summary of Prototype Data.

Authorization to make these tests in the High Speed Water Tunnel of the Hydrodynamics Laboratory at the California Institute of Technology was contained in a letter from Dr. E. H. Colpitts, Chief of Section 6.1, National Defense Research Committee, dated April 9, 1945.

The purpose of the tests was to determine the hydrodynamic characteristics, cavitation parameters and suitability of the 10-degree cone angle shroud ring.

Figure 2 also shows a profile of this ring. The 5-degree *half* cone angle is indicated. The 5-degree cone angle ring, also tested, had the same profile but was set at *half* the angle shown. The profile dimensions of these rings are given under Summary of Prototype Data.

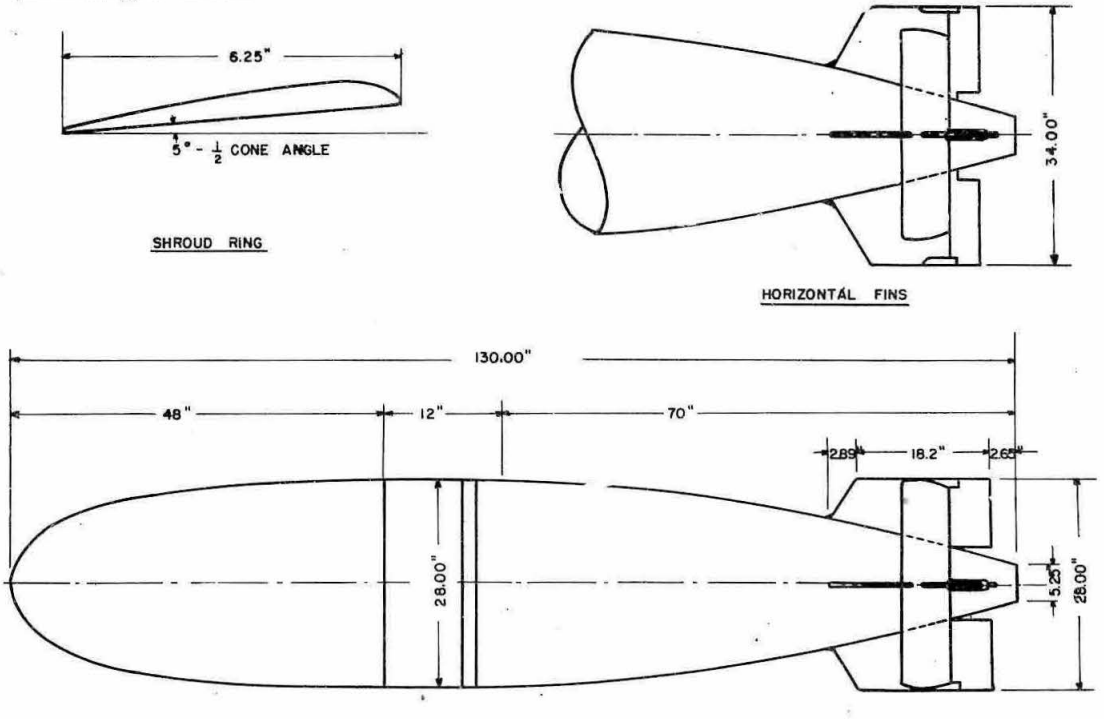

FIG. 2 — OUTLINE DRAWING OF UNITED SHOE MACHINERY CORPORATION NO. 8 HYDROBOMB

SUMMARY OF PROTOTYPE DATA

Over-all length	130 inches
Body diameter	28 inches
Fin span	(a) vert. 28 in., horiz. 28 in.
	(b) vert. 28 in., horiz. 34 in.
Weight, with fuel	3500 pounds
Total displacement	32.15 cubic feet
Designed speed	70 miles per hour
Normal operating depth	15 feet
Center of gravity	60 inches from nose

U. S. M. C. Hydrobomb, Design No. 8

NOSE CONTOUR		AFTERBODY CONTOUR		SHROUD RING	
L	D	L	D	L'	O.D.
0	0	60	28.000	0	27.546
1	8.358	66	27.860	.350	27.930
2	11.344	70	27.606	.700	27.950
4	15.100	74	27.198	1.050	27.983
6	17.616	78	26.624	1.400	27.997
8	19.500	82	25.872	1.537	28.000
10	20.982	86	24.940	1.750	27.996
12	22.181	90	23.824	2.100	27.978
16	24.006	94	22.526	2.450	27.941
20	25.294	98	21.058	2.800	27.888
24	26.220	102	19.426	3.150	27.815
28	26.884	106	17.646	3.500	27.724
32	27.350	110	15.736	3.850	27.615
36	27.666	114	13.724	4.200	27.876
40	27.864	118	11.636	4.550	27.342
44	27.968	122	9.502	4.900	27.178
48	28.000	126	7.360	5.250	26.996
		130	5.250	5.600	26.810
				5.950	26.592
				6.250	26.307

L = distance from nose tip, inches

D = diameter, inches

L' = distance from forward edge of ring, inches

O.D. = outside diameter, inches

TESTS MADE

1. Finless Models

   A. Polarized Light Flume flow study around rear end of afterbody.

   B. Amount and variation of drag, cross force, and moment (about center of gravity) coefficients (C_D, C_C, and C_M) at angles of yaw from 0 to 10 degrees, inclusive.

   C. Amount and variation of drag coefficient with Reynolds number.

2. Finned Models *without* Shroud Rings

   A. Polarized Light Flume diagrams for afterbodies at 0 and 10 degrees yaw.

   B. Drag, cross force, and moment coefficient determinations for yaw angles 0 to ± 10 degrees for neutral rudders and vertical rudders at 10 degrees port.

   C. Drag, lift, and moment coefficient determinations for pitch angles 0 to ± 10 degrees for neutral rudders and horizontal rudders at 5 and 10 degrees down.

   D. Amount and variations of drag coefficient with Reynolds number.

   E. Determination of incipient cavitation values for nose, body, and fins.

3. Models with 10- and 5-degree Cone Angle Shroud Rings

   A. Full model flow diagrams, 0 and 10-degrees yaw, for model with 28-inch fins and 10-degree ring; afterbody diagrams for the model with 34-inch fins, 10-degree ring, and model with 34-inch fins and 5-degree ring.

   B. Same as 2 B

   C. Same as 2 C

   D. Same as 2 D

   E. Same as 2 E but with incipient cavitation with rings added.

All force and moment coefficients contained in this report have been corrected for shield interference. The drag measurements have been corrected for horizontal buoyancy or pressure drop in the tunnel working section. The symbols used in the report are defined in the appendix.

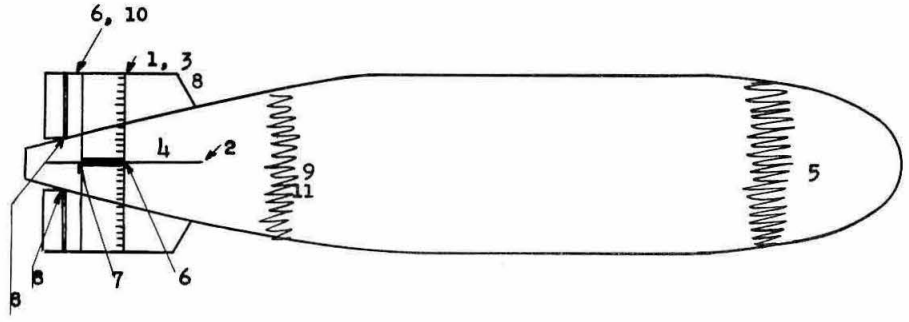

ORDER	K	LOCATION
1	0.36	Leading edge of shroud ring, 28" fin span model
2	0.33	Streaks on leading dege of starboard horizontal fin, 34" fin span model, probably due to irregularities
3	0.32	Leading edge of shroud ring, 34" fin span model
4	0.29	Horizontal rudder, nearly full surface, 34" fin span model
5	0.27	Average value, nose
6	0.24	Leading edge of starboard bracket joining horizontal fin and rudder, also vertical fin and rudder, both for 34" fin span model
7	0.22	Trailing edge of lug joining horizontal fin and rudder, 28" fin span model
8	0.21	Leading edge of vertical fins and rudder post connections, 34" fin span model
9	0.20	Afterbody, 34" fin span model
10	0.19	Leading edge of lug joining vertical rudder and fin, 28" fin span model
11	0.18	Afterbody, 28" fin span model

All values for incipient cavitation. Parameters for incipient cavitation for hydrobomb with 10° cone angle shroud ring.

FIG. 3 – CAVITATION PARAMETERS

RESULTS OBTAINED AND DISCUSSION

1. CAVITATION

Figure 3 is a diagram and list showing the order and location of incipient cavitation for the models with the 10-degree cone angle ring. Cavitation began on the inner side of the 5-degree ring at an average K value of 0.90, and was about 1/8-inch wide thereat for K = 0.55. Cavitation for other parts of these models was sensibly unchanged from those shown on Figure 3.

The value of K for a speed of 70 miles per hour at 15 feet submergence is 0.295.

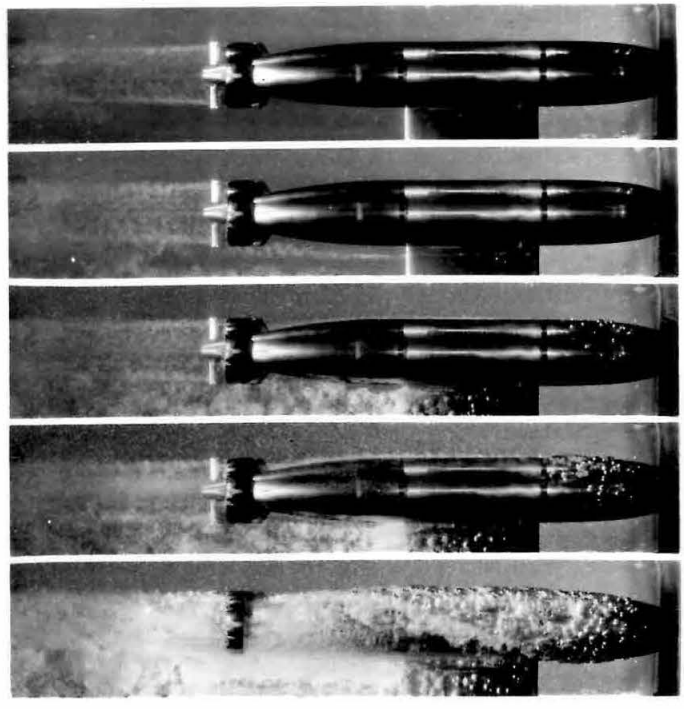

FIG. 4 — CAVITATION DEVELOPMENT ON HYDROBOMB WITH 28-INCH FIN SPAN AND 5-DEGREE CONE ANGLE SHROUD RING

Cavitation data may be summarized thus:

MODEL	28" FIN SPAN	34" FIN SPAN
Shroud ring, 5° (average value)	0.90	0.90
10° (average value)	0.34	0.34
Horizontal fins	-	0.33
Horizontal rudder	-	0.29
Nose (average value)	0.27	0.27
Afterbody (average value)	0.22	0.22
Vertical fins	-	0.21

Values which have been changed from those in a preliminary Memorandum Report are based on averages from additional runs.

Figure 4 shows the character and progressive development of cavitation for the hydrobomb with 28-inch fin span and 5-degree cone ring. Cavitation photographs were not taken at the time the 10-degree cone ring models were tested, but the characteristics were similar except for the increased cavitation from the inner surface of the ring here shown.

A submergence chart, suitable for this projectile, appears as Figure 20. This chart gives the values of K corresponding to any submergence and velocity in the operating range for the hydrobomb. See appendix for further discussion.

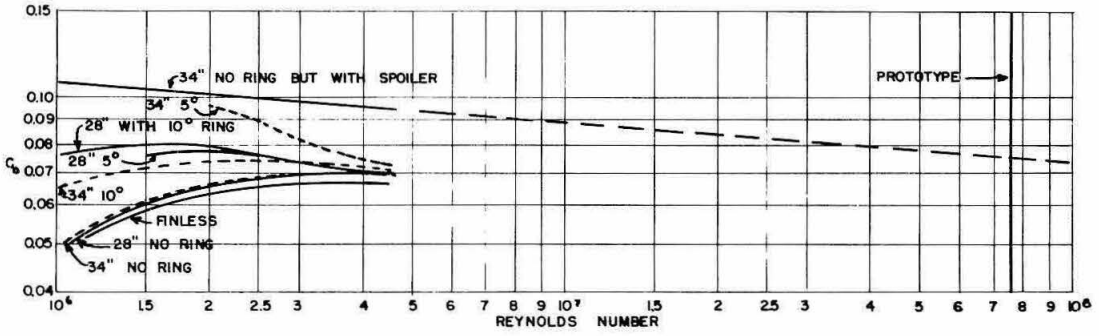

FIG. 5 – DRAG COEFFICIENT FOR USMC HYDROBOMB, DESIGN NO. 8

2. DRAG COEFFICIENT AGAINST REYNOLDS NUMBER

Figure 5 indicates the relationship of the drag coefficient of these models to Reynolds number. With two exceptions, there is evidence in these curves that the drag coefficient, C_D, for Reynolds numbers below about 3×10^6, follows a transition curve between those for laminar and turbulent flow, the latter condition being obtained for higher R values. The topmost curve was obtained for check purposes by placing an 0.018-inch diameter spoiler wire on the nose of the 34-inch fin span model with no shroud ring to insure turbulent flow at all test velocities. The second curve from the top, for the 34-inch fin span model with 5-degree cone angle ring is believed to be of dubious value due to inconsistencies in the data obtained. The cause of these inconsistencies has not been determined at present. This difficulty was not encountered with other models. The maximum velocity available in the Water Tunnel is insufficient to establish clearly the trend of values to prototype Reynolds numbers, but it appears reasonable to assume that their C_D under design conditions would be about 0.05.

3. YAW ANGLE EFFECTS

Figure 6 shows the effect of ± 10 degrees of yaw angle on the drag coefficient, C_D, for all seven models. The effect of 10-degree port rudder is also shown for all finned models. The curves for neutral rudders are symmetrical and those for 10-degree rudders cross as would be anticipated from the asymmetry introduced, except in the case of the model with 28-inch fin span and 5-degree cone angle ring. The reason for the odd results with this model is not understood.

Figure 7 is similar to Figure 6 except that the cross force coefficient, C_C, is represented instead of C_D. The lines for the shroudless models are curved while those with shrouds are straight.

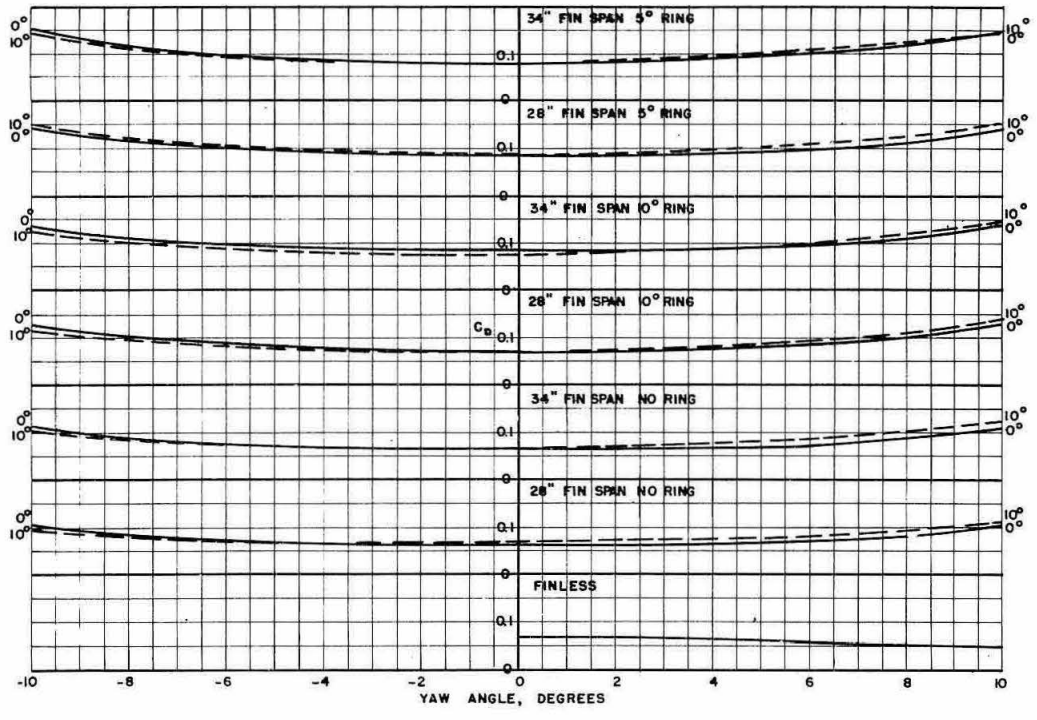

FIG. 6 — USMC HYDROBOMB, DESIGN NO. 8
DRAG COEFFICIENT, C_D, AGAINST YAW ANGLE
Horizontal Rudders 0°

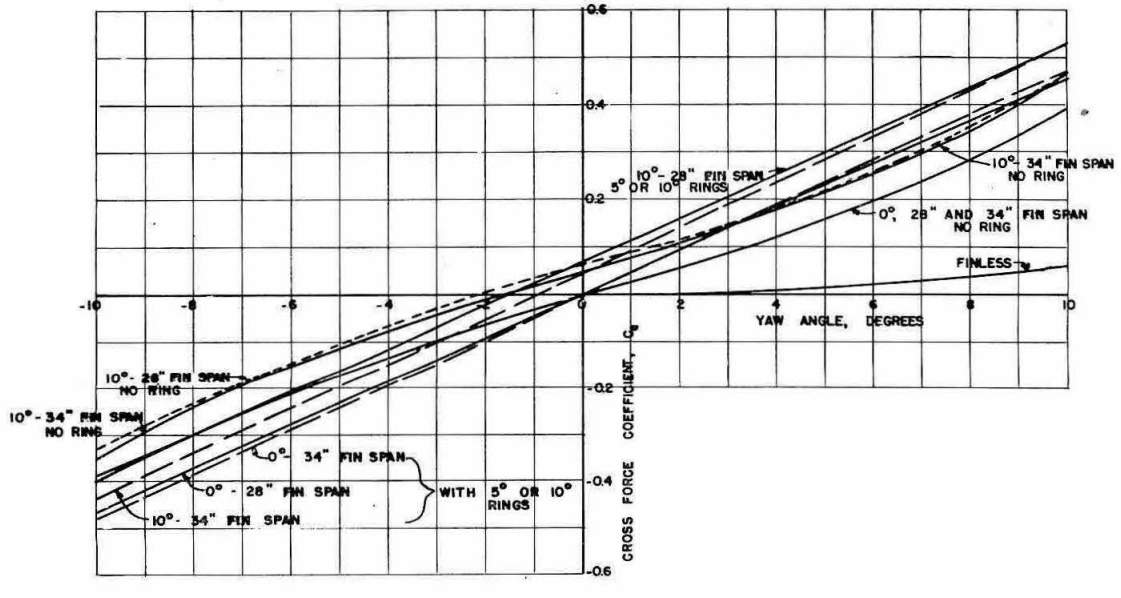

FIG. 7 — CROSS FORCE COEFFICIENT CURVES FOR HYDROBOMB
WITH VARIOUS COMBINATIONS OF FINS, SHROUD RINGS
AND RUDDER SETTINGS

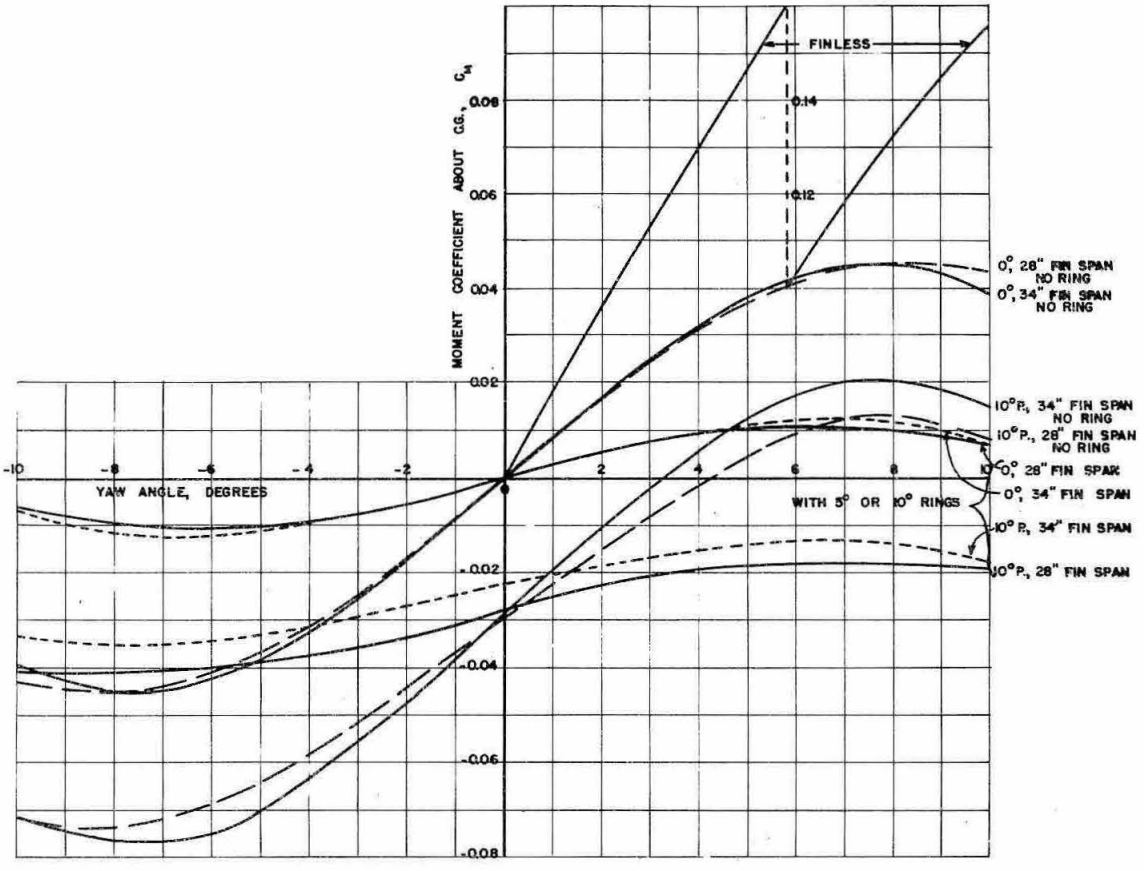

FIG. 8 – INFLUENCE OF YAW ANGLE ON MOMENT COEFFICIENT FOR FINLESS, RINGLESS, AND 10° CONE ANGLE RINGS

Any differences in cross force coefficient between the 28-inch fin span models with 10 and 5-degree rings or between the 34-inch fin span models with 10 and 5-degree rings are within the errors of measurement. As a result, the curves marked "with ring" apply to either shroud ring. In each case there is a 0 and a 10-degree port rudder curve but the 0-degree curve for both shroudless models is identical within limits of measurement. The curves for 10-degree rudders for the shroudless models are not quite identical, the 28-inch fin span model showing slightly greater cross force coefficient. The straight lines for the ring tail models, with neutral rudders, are at a slight angle with each other, the 28-inch fin span model showing a smaller C_C, in this case. When rudders are at 10 degrees, the C_C of the 28-inch fin span model is, again, greater. Rudder action materially increases C_C and the effect of all rudders in this design is several times that of the rudders of the 30-A design previously tested.* The effect of the shroud ring on C_C is to increase it and make it directly proportional to the yaw angle.

*"Water Tunnel Tests of the Hydrobomb", Report Section 6.1-sr207-1276 by H. L. Doolittle, May 13, 1944.

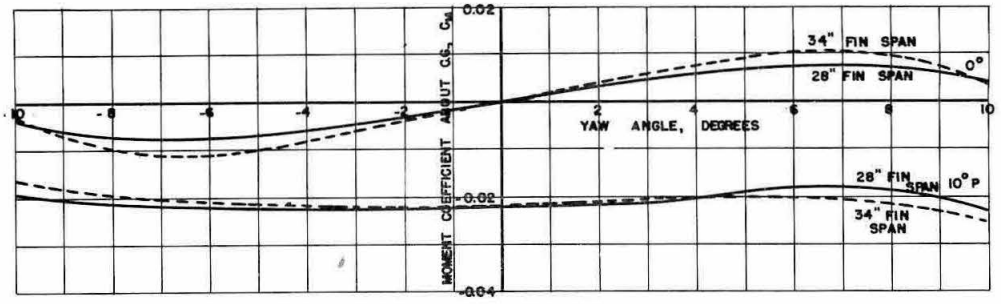

FIG. 9 – INFLUENCE OF YAW ANGLE ON MOMENT COEFFICIENT FOR 5° CONE ANGLE RING MODELS

Horizontal Rudders 0°

Figures 8 and 9 are similar to the two previous except that the moment coefficient about the center of gravity, C_M, is now represented as a function of yaw. The moment of the finless model shown in Figure 8 was so much greater than for the other models, that the curve ran off the paper. The larger moments have been included in the upper right corner by use of the supplementary scale, i.e., the curve has been dropped by the length of the vertical dash line. The 0-degree rudder curves for the shroudless models pass through the origin at an angle of approximately 40 degrees with the horizontal axis and are nearly identical. The 10-degree port rudder setting creates a large negative moment, displacing the curves downward. The addition of the 10-degree cone angle rings makes the hydrobomb almost statically stable against yaw, as indicated by the small angles the curves make with the horizontal axis. The rudder effect is larger for the 28-inch fin span model with 10-degree ring than for the 34-inch fin span model with 10-degree ring. By comparing Figures 8 and 9 it may be seen that the 5-degree cone angle rings give approximately the same C_M values as the 10-degree rings when rudders are neutral, but a 10-degree port rudder produces a moment curve which is nearly horizontal for both the 28-inch and 34-inch fin span models.

4. PITCH ANGLE EFFECTS

Figure 10 is similar to Figure 6 except the variation of drag coefficient is shown with pitch angle instead of yaw angle, and the horizontal rudder effect was obtained instead of that of the vertical rudders. Tests were made with horizontal rudders at 0, 5, and 10 degrees down. The effect of the 5-degree down rudder on the drag coefficient was, in general, difficult to measure as the differences from zero rudder were small. They are shown when noted. The 10-degree rudder effect was more pronounced. Curves for neutral rudder were again symmetrical. The 10-degree curves cross the 0-degree curves except in the case of the 28-inch fin span, 5-degree model, for an undetermined reason.

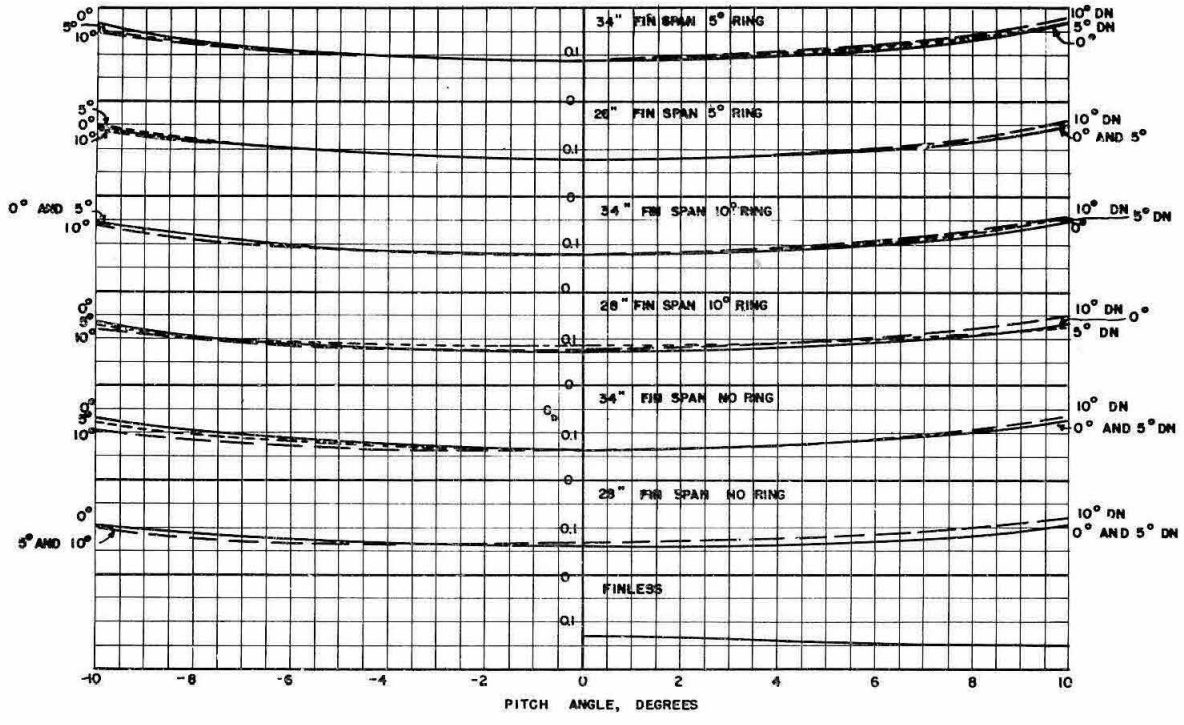

FIG. 10 — DRAG COEFFICIENT, C_D, AGAINST PITCH ANGLE

Vertical Rudders 0°

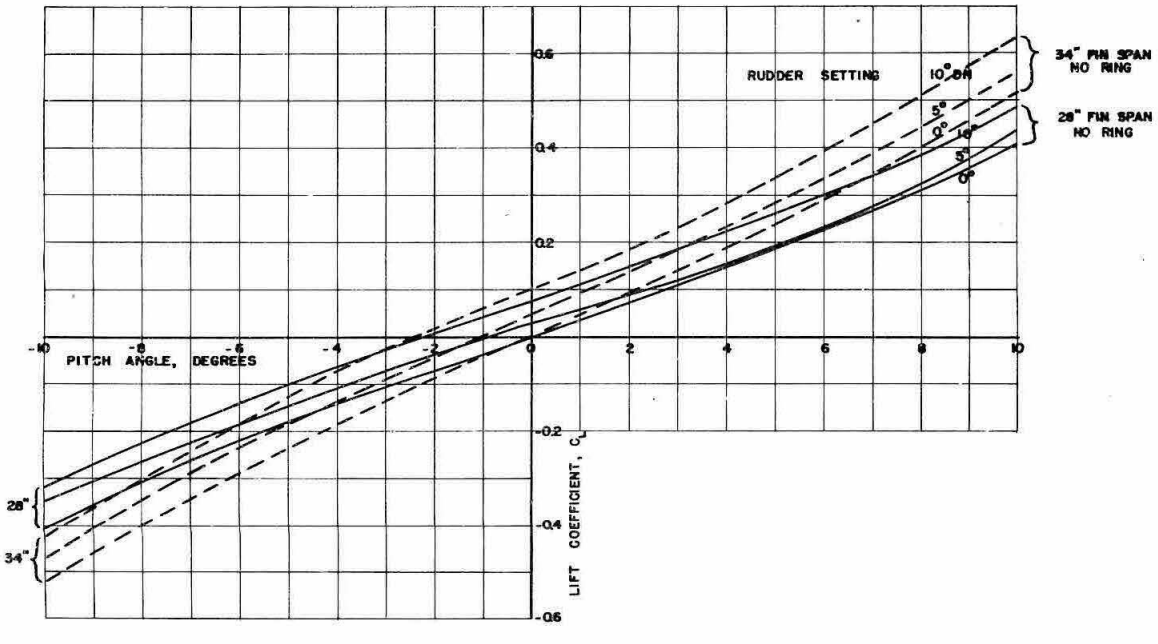

FIG. 11 — INFLUENCE OF PITCH ANGLE ON LIFT COEFFICIENT

ON MODELS WITHOUT RINGS

Vertical Rudders 0°

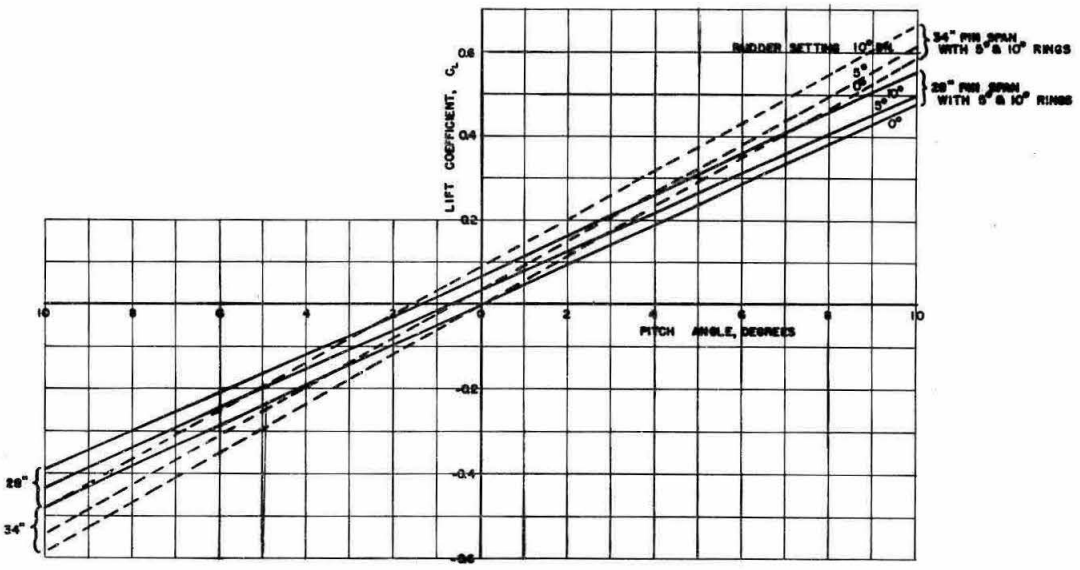

FIG. 12 – INFLUENCE OF PITCH ANGLE ON LIFT COEFFICIENT ON MODELS WITH 5° AND 10° RINGS
Vertical Rudders 0°

Figure 11 shows the effect of positive and negative pitch angles on the lift coefficient, C_L, for the shroudless models. Unbroken lines are for the 28-inch fin span model; dash lines for the 34-inch fin span model. Horizontal rudder settings of 0, 5, and 10 degrees down are given and, as may be noted, the lines are not straight. The rudders of the 34-inch fin span model have the greater effect on C_L. Figure 12 is the same as Figure 11 except the models have shroud rings. Any differences in these curves for 10 or 5-degree cone angle rings is within the limits of measurement and, hence, the curves represent both rings. The effect of the rings on the lift coefficient is, as was seen for the cross force coefficient, to convert the curves to straight lines. There is an increase in the values at the extremes. The intermediate 5-degree down rudder effect is much greater on the lift (Figures 11 and 12) than on the drag (Figure 10).

Figures 13 and 14 show the effect of pitch angle on the moment coefficient about the center of gravity. It is apparent that the 28-inch fin span model without ring has the greatest amount of static instability; the 34-inch fin span model without ring has about half as much; the 28-inch fin span model with either ring has curves which are sensibly parallel to the pitch axis; and the 34-inch fin span model with either ring has marked static stability.

The fin and rudder area of the No. 8 Design Hydrobomb is more than 50 per cent greater even with the 28-inch fins than those of the Mk 13 Torpedo.* The addition of shroud rings produces effects

*"Water Tunnel Tests of the Mk 13-1, Mk 13-2, and Mk13-2A Torpedoes," OSRD No. 6-1-sr207-936 by Joseph Levy, November 9, 1943.

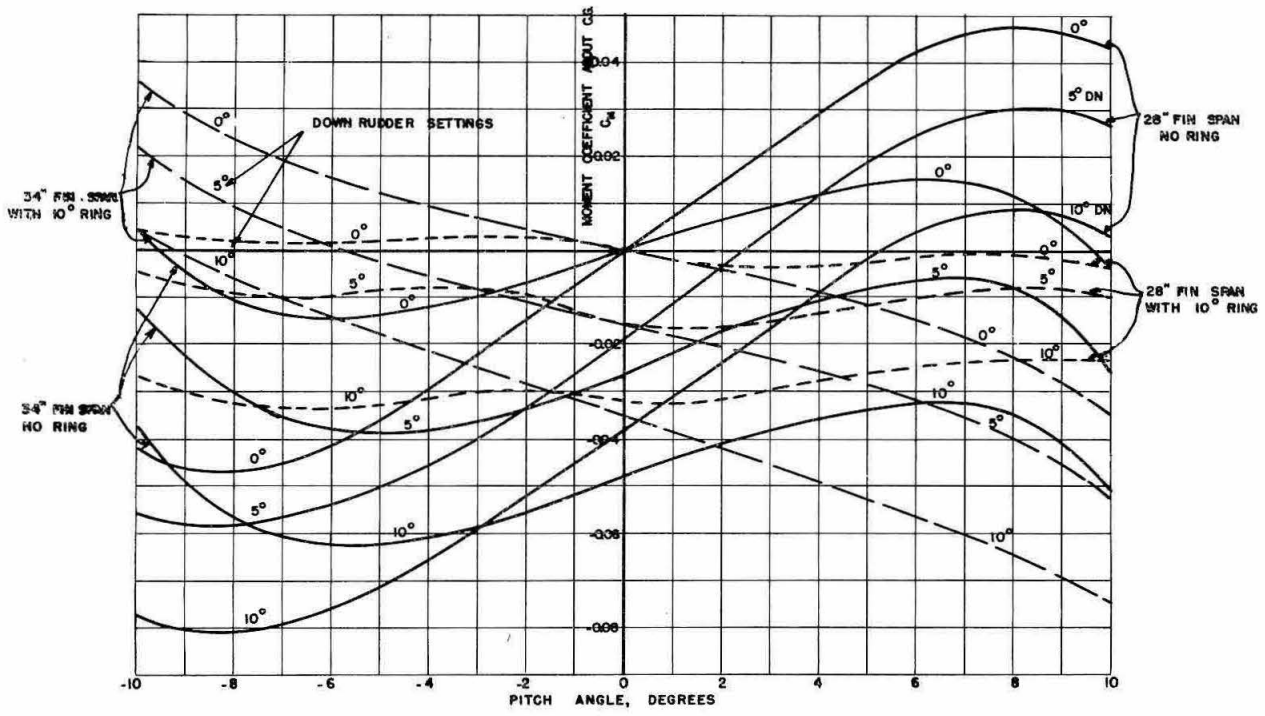

FIG. 13 – INFLUENCE OF PITCH ANGLE ON MOMENT COEFFICIENT AT VARIOUS HORIZONTAL RUDDER SETTINGS RINGLESS AND 10° MODELS

Vertical Rudders 0°

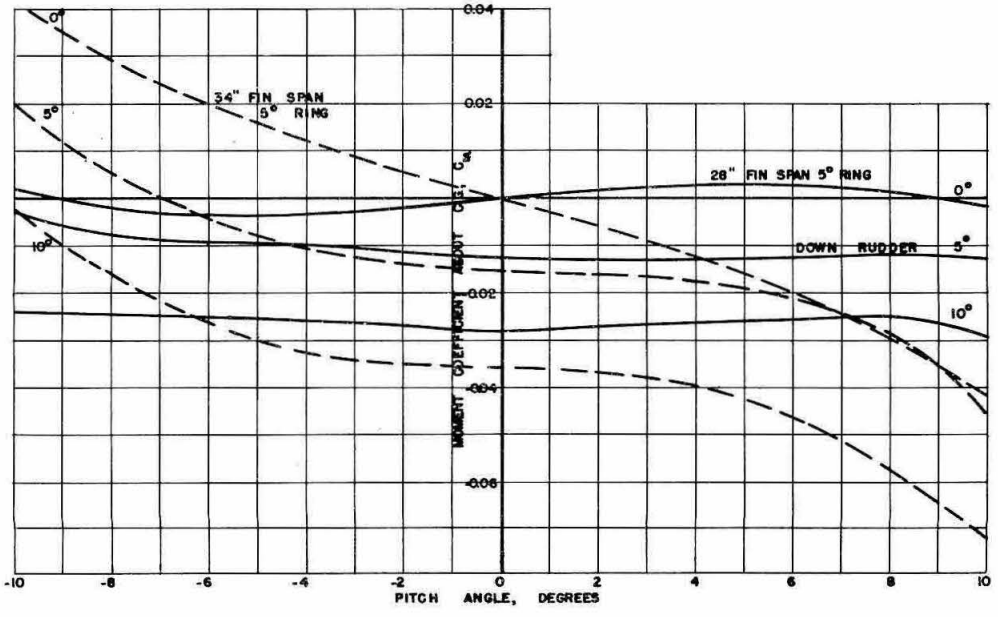

FIG. 14 – INFLUENCE OF PITCH ANGLE ON MOMENT COEFFICIENT FOR MODELS WITH 5° RING

Vertical Rudders 0°

which limit their usefulness to the bubble stage. Static instability is desirable for proper control and maneuverability. The design with four fins of 28-inch fin span accordingly seems to be preferable, and the advantage of any shroud ring therewith worthy of further investigation.

5. FLOW DIAGRAMS

Figures 15 and 16 are qualitative diagrams of the flow patterns over the afterbody and tail surfaces of the 28-inch and 34-inch fin span shroudless models, respectively, at 0 and 10 degrees of yaw. The only observable difference noted in flow patterns of these models was an increased disturbance on the upper surface of the 34-inch horizontal fins at 10-degrees yaw, probably due to their greater size.

Figure 17 is the flow diagram for the 34-inch fin afterbody with 10-degree ring (0 and 10-degrees yaw), and Figure 18 gives the flow patterns for the complete model with 28-inch fins and 10-degree ring at similar yaws. The nose and main body patterns are the same for all afterbodies and tails. The addition of shroud rings produces an unusually complicated, swirling flow pattern over the vanes and along the adjacent body, especially at 10-degrees yaw which cannot be shown in the drawings.

Figure 19 shows the relationship of the 5-degree ring to the adjacent flow. No difference was noted between 28-inch and 34-inch fin span models in this respect. The cross-sectional design of this ring appears to be unsuited to this angle of attack, separations occurring on both top and bottom surfaces.

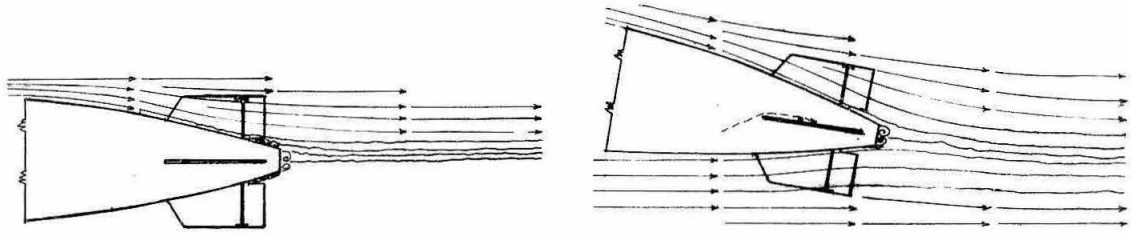

YAW = 0° YAW = 10°

FIG. 15 - 28-INCH FIN SPAN WITHOUT RING

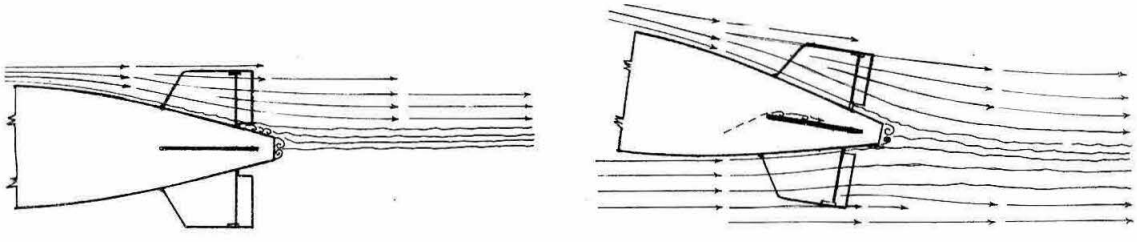

YAW = 0° YAW = 10°

FIG. 16 - 34-INCH FIN SPAN WITHOUT RING

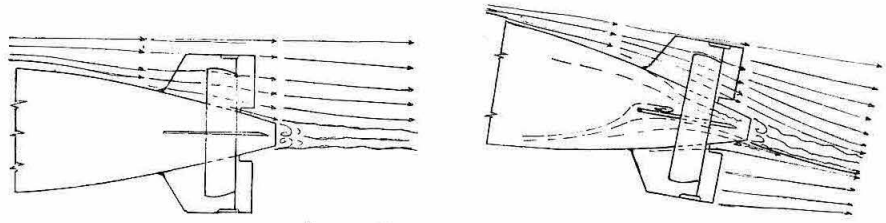

YAW = 0° YAW = 10°

FIG. 17 - 34-INCH FIN SPAN WITH 10° RING

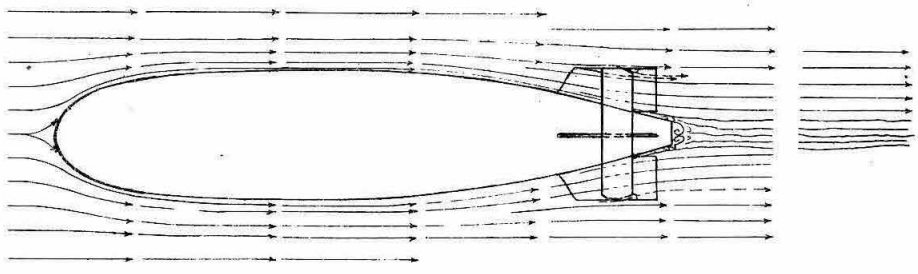

YAW = 0°

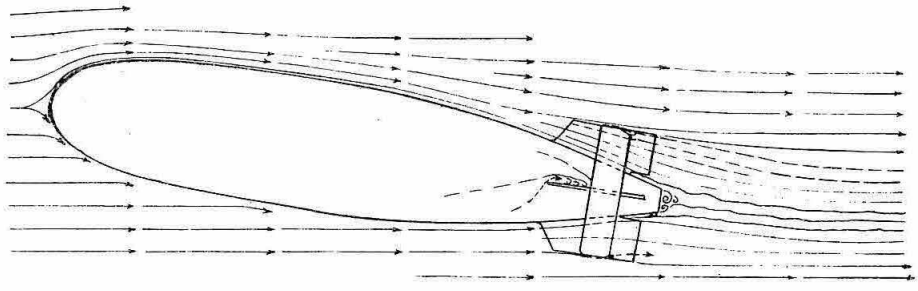

YAW = 10°

FIG. 18 - 28-INCH FIN SPAN WITH 10° RING

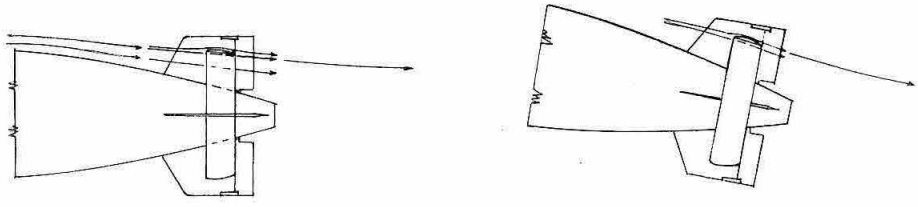

YAW = 0° YAW = 10°

FIG. 19 - 34-INCH FIN SPAN WITH 5° RING

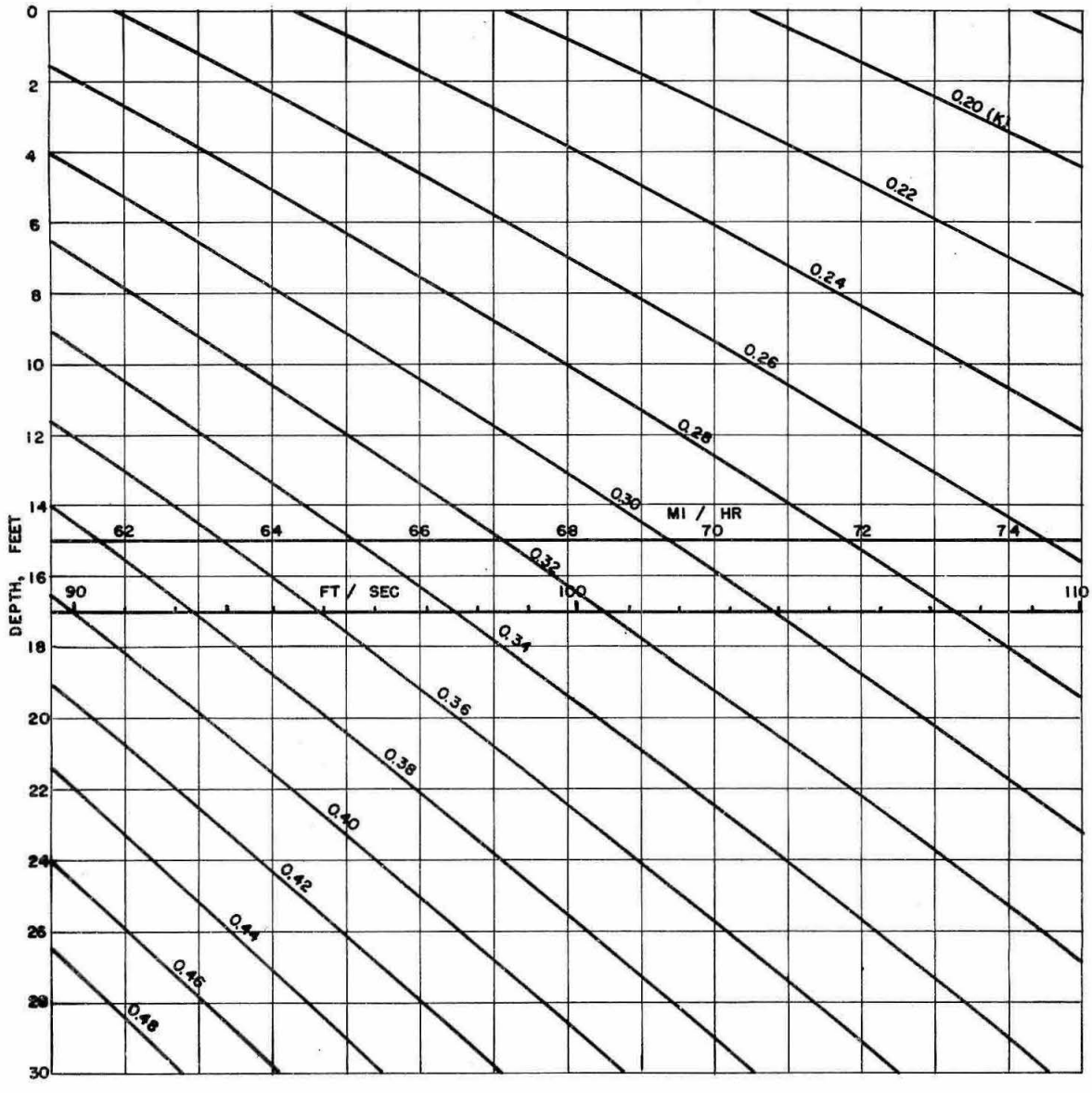

FIG. 20 — SUBMERGENCE CHART FOR SEA WATER

APPENDIX

DEFINITIONS

YAW ANGLE, ψ

The angle, in a horizontal plane, which the axis of the projectile makes with the direction of motion. Looking down on the projectile, yaw angles in a clockwise direction are positive (+) and in a counterclockwise direction, negative (−).

PITCH ANGLE, α

The angle, in a vertical plane, which the axis of the projectile makes with the direction of motion. Pitch angles are positive (+) when the nose is up and negative (−) when the nose is down.

LIFT, L

The force, in pounds, exerted on the projectile normal to the direction of motion and in a vertical plane. The lift is positive (+) when acting upward and negative (−) when acting downward.

CROSS FORCE, C

The force, in pounds, exerted on the projectile normal to the direction of motion and in a horizontal plane. The cross force is positive when acting in the same direction as the displacement of the projectile nose for a positive yaw angle, i.e., to an observer facing in the direction of travel, a positive cross force acts to the right

DRAG, D

The force, in pounds, exerted on the projectile parallel with the direction of motion. The drag is positive when acting in a direction opposite to the direction of motion

MOMENT, M

The torque, in foot pounds, tending to rotate the projectile about a transverse axis. Yawing moments tending to rotate the projectile in a clockwise direction (when looking down on the projectile) are positive (+), and those tending to cause counterclockwise rotation are negative (−). Pitching moments tending to rotate the projectile in a clockwise direction (when looking at the projectile from the port side) are positive (+), and those tending to cause counterclockwise rotation are negative (−).

In accordance with this sign convention a moment has a destabilizing effect when it has the same sign as the yaw angle or pitch angle, and a stabilizing effect when the moment and yaw or pitch angle have opposite signs

NORMAL COMPONENT, N

The sum of the components of the drag and cross force (or lift) acting normal to the axis of the projectile. The value of the normal component is given by the following:

$$N = D \sin \psi + C \cos \psi \qquad (1)$$

or

$$N = D \sin \alpha + L \cos \alpha \qquad (1a)$$

in which

N = Normal component in lbs

D = Drag in lbs

C = Cross force in lbs

L = Lift force in lbs

ψ = Yaw angle in degrees

α = Pitch angle in degrees

CENTER OF PRESSURE, CP

The point in the axis of the projectile at which the resultant of all forces acting on the projectile is applied.

CENTER-OF-PRESSURE ECCENTRICITY, e

The distance between the center of pressure (CP) and the center of gravity (CG) expressed as a decimal fraction of the length (l) of the projectile. The center-of-pressure eccentricity is derived as follows:

$$e = (l_{cp} - l_{cg}) \frac{1}{l} = \frac{1}{l} \frac{M_{cg}}{N} \qquad (2)$$

in which

e = Center-of-pressure eccentricity

l = Length of projectile in feet

l_{cg} = Distance from nose of projectile to CG in feet

l_{cp} = Distance from nose of projectile to CP in feet

COEFFICIENTS

The force and moment coefficients used are derived as follows:

Drag coefficient, $$C_D = \frac{D}{\rho \frac{V^2}{2} A_D} \quad (3)$$

Cross force coefficient, $$C_C = \frac{C}{\rho \frac{V^2}{2} A_D} \quad (4)$$

Lift coefficient, $$C_L = \frac{L}{\rho \frac{V^2}{2} A_D} \quad (5)$$

Moment coefficient, $$C_M = \frac{M}{\rho \frac{V^2}{2} A_D l} \quad (6)$$

in which

D = Measured drag force in lbs

C = Measured cross force in lbs

L = Measured lift force in lbs

ρ = Density of the fluid in slugs/cu ft = w/g

w = Specific weight of the fluid in lbs/cu ft

g = Acceleration of gravity in ft/sec^2

A_D = Area in sq ft at the maximum cross section of the projectile taken normal to the geometric axis of the projectile

V = Mean relative velocity between the water and the projectile in ft/sec

M = Moment, in foot-pounds, measured about any particular point on the geometric axis of the projectile

l = Overall length of the projectile in feet

RUDDER EFFECT

The total increase or decrease in moment coefficient, at a given yaw or pitch angle, resulting from a given rudder setting. This increase or decrease in moment coefficient is measured from the moment coefficient curve for neutral rudder setting.

REYNOLDS NUMBER

In comparing hydraulic systems involving only friction and inertia forces, a factor called Reynolds number is of great utility. This is defined as follows:

$$R = \frac{lV}{\nu} = \frac{lV\rho}{\mu} \qquad (7)$$

in which

R = Reynolds number

l = Overall length of projectile, feet

V = Velocity of projectile, feet per sec

ν = Kinematic viscosity of the fluid, sq ft per sec = μ/ρ

ρ = Mass density of the fluid in slugs per cu ft

μ = Absolute viscosity in pound-seconds per sq ft

Two geometrically similar systems are also dynamically similar when they have the same value of Reynolds number. For the same fluid in both cases, a model with small linear dimensions must be used with correspondingly large velocities. It is also possible to compare two cases with widely differing fluids provided l and V are properly chosen to give the same value of R.

CAVITATION PARAMETER

In the analysis of cavitation phenomena, the cavitation parameter has been found very useful. This is defined as follows:

$$K = \frac{p_L - p_B}{\rho \frac{V^2}{2}} \qquad (8)$$

in which

K = Cavitation parameter

p_L = Absolute pressure in the undisturbed liquid, lbs/sq ft

p_B = Vapor pressure corresponding to the water temperature, lbs/sq ft

V = Velocity of the projectile, ft/sec

ρ = mass density of the fluid in slugs per cu ft = w/g

w = weight of the fluid in lbs per cu ft

g = acceleration of gravity

Note that any homogeneous set of units can be used in the computation of this parameter. Thus, it is often convenient to express this parameter in terms of the head, i.e.,

$$K = \frac{h_L - h_B}{\frac{V^2}{2g}} \qquad (9)$$

where

h_L = Submergence plus the barometric head, ft of water

h_B = Pressure in the bubble, ft of water

It will be seen that the numerator of both expressions is simply the net pressure acting to collapse the cavity or bubble. The denominator is the velocity pressure. Since the entire variation in pressure around the moving body is a result of the velocity, it may be considered that the velocity head is a measure of the pressure available to open up a cavitation void. From this point of view, the cavitation parameter is simply the ratio of the pressure available to collapse the bubble to the pressure available to open it. If the K for incipient cavitation is considered, it can be interpreted to mean the maximum reduction in pressure on the surface of the body measured in terms of the velocity head. Thus, if a body starts to cavitate at the cavitation parameter of one, it means that the lowest pressure at any point on the body is one velocity head below that of the undisturbed fluid.

The shape and size of the cavitation bubbles for a specific projectile are functions of the cavitation parameter. If p_B is taken to represent the gas pressure within the bubble instead of the vapor pressure of the water, as in normal investigations, the value of K obtained by the above formula will be applicable to an air bubble. In other words, the behavior of the bubble will be the same whether the bubble is due to cavitation, the injection of exhaust gas, or the entrainment of air at the time of launching.

The cavitation parameter for incipient cavitation has the symbol K_i.

The following chart gives values of the cavitation parameter as a function of velocity and submergence in sea water.

GENERAL DISCUSSION OF STATIC STABILITY

Water tunnel tests are made under steady flow conditions, consequently the results only indicate the tendency of the steady state hydrodynamic couples and forces to cause the projectile to return to or move away from its equilibrium position after a

disturbance. Dynamic couples and forces including either positive or negative damping are not obtained. If the hydrodynamic moments are restoring the projectile, then it is said to be statically stable; if nonrestoring, statically unstable. In the discussion of static stability the actual motion following a perturbation is not considered at all. In fact, the projectile may oscillate continuously about an equilibrium position without remaining in it. In this case it would be statically stable, but would have zero damping and hence, be dynamically unstable. With negative damping a projectile would oscillate with continually increasing amplitude following an initial perturbation even though it were statically stable. Equilibrium is obtained if the sum of the hydrodynamic, buoyant, and propulsive moments equal zero. In general, propulsive thrusts act through the center of gravity of the projectile so only the first two items are important.

If a projectile is rotating from its equilibrium position so as to increase its yaw angle positively, the moment coefficient must increase negatively (according to the sign convention adopted) in order that it be statically stable. Therefore, for projectiles without controls or with fixed control surfaces, a negative slope of the curve of moment coefficient vs yaw gives static stability and a positive slope gives instability. For a projectile without controls, static stability is necessary for a successful flight unless stability is obtained by spinning as in the case of rifle shells. For a projectile with controls, stabilizing moments can be obtained by adjusting the control surfaces, and the slope of the moment coefficient, as obtained with fixed rudder position, need not give static stability. Where buoyancy either acts at the center of gravity or can be neglected, equilibrium is obtained when the hydrodynamic moment coefficient equals zero. For symmetrical projectiles this occurs at zero yaw angle, i.e., when the projectile axis is parallel to the trajectory. For nonsymmetrical projectiles, such as a torpedo when the rudders are not neutral, the moment is not zero at zero yaw but vanishes at some definite angle of attack. Where buoyancy cannot be neglected equilibrium is obtained when $C_{l} = -C_{l_{buoyancy}}$, and the axis of the projectile is at some angle with the trajectory.

For symmetrical projectiles the degree of stability or instability can be obtained from the center of pressure curves. If the center of pressure falls behind the center of gravity, a restoring moment exists giving static stability. If the center of pressure falls ahead of the center of gravity, the moment is nonrestoring, and the projectile will be statically unstable. The degree of stability or instability is indicated approximately by the distance between the center of gravity and the center of pressure. In general, for nonsymmetrical projectiles, the cross force or lift is not zero when the moment vanishes so that the center of pressure curve is not symmetrical and the simple rules just stated cannot be used to determine whether or not the projectile will be stable. In such cases careful interpretation of the moment curves is a more satisfactory method of determining stability relationship.

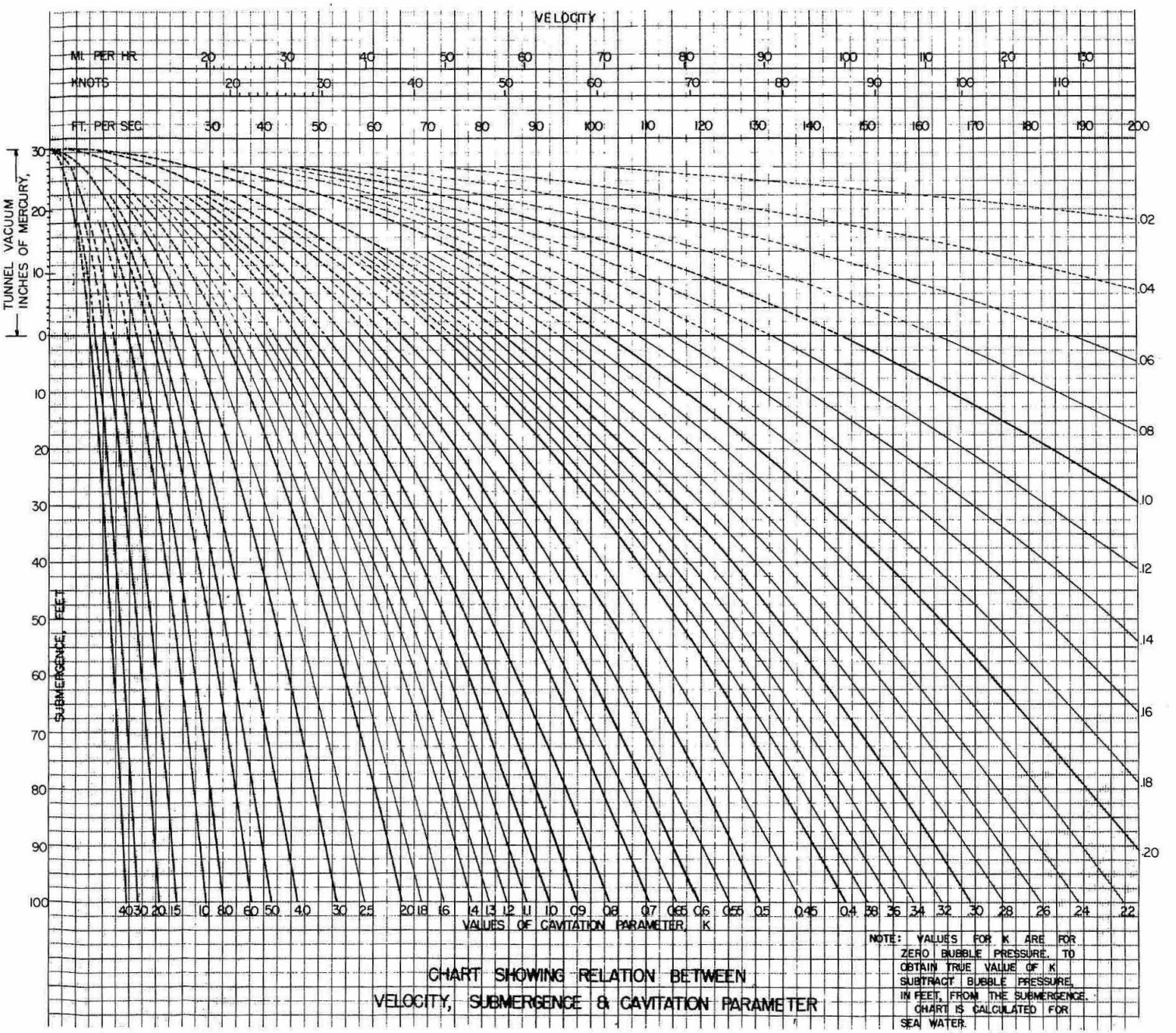

CHART SHOWING RELATION BETWEEN VELOCITY, SUBMERGENCE & CAVITATION PARAMETER